DEVELOPING A PHANTOM FOR THE POSITRONIUM IMAGING EVALUATION*

G. Łapkiewicz, Sz. Niedźwiecki, P. Moskal

on behalf of the J-PET Collaboration

Faculty of Physics, Astronomy and Applied Computer Science
Jagiellonian University, Cracow, Poland
and
Center for Theranostics, Jagiellonian University, Cracow, Poland
and
Total-Body Jagiellonian-PET Laboratory, Jagiellonian University
Cracow, Poland

Received 16 October 2022, accepted 25 October 2022, published online 15 November 2022

In this contribution, a concept for a new phantom for positronium imaging with PET scanners is described. The proposed phantom is based on the NEMA IEC phantom in which six high-activity spheres are filled with solutions characterized by a different mean ortho-positronium lifetime. A method for controlling ortho-positronium lifetime is discussed along with preliminary results. The XAD4 suspended in various fractions of water was tested as a potential model of a sample with a controlled mean lifetime of ortho-positronium. The mean lifetime of ortho-positronium for six samples was estimated by means of the Positronium Annihilation Lifetime Spectroscopy (PALS). Obtained spectra were fitted with the PALS Avalanche analysis program and components corresponding to the ortho-positronium annihilation in the XAD4 pores were established. As a result, the correlations between the lifetime and production intensity of ortho-positronium and the concentration of XAD4 in water were determined.

DOI:10.5506/APhysPolBSupp.15.4-A4

1. Introduction

The positronium imaging method was invented and is being developed at the Jagiellonian University [1–6]. It utilizes positronium bound-state lifetime information to provide additional insight into internal structure of the

* Presented at the 4th Jagiellonian Symposium on *Advances in Particle Physics and Medicine*, Cracow, Poland, 10–15 July, 2022.

studied objects and is promising as a tool for raising the specificity of medical diagnostics [5, 7]. This method can be applied in the PET examination, but unlike a standard PET procedure, it involves registration of more than two annihilation gamma quanta [2–4]. To perform that, it is necessary to adjust the scanner for multiphoton detection. The first scanner with that ability, J-PET, was constructed at the Jagiellonian University [8, 9].

Based on an *ex vivo* study conducted using positronium imaging, it is anticipated that inside the patient's body, about 40% of positron annihilation can occur through the production of positronium [2, 10]. Most of the ortho-positronia annihilate by the emission of two photons by the pick-off process [11] and ortho–para conversion [12–14]. In the first case, positron from ortho-positronium annihilates with an electron from surrounding matter, in the latter case, interaction of ortho-positronium with surrounding molecules leads to conversion of ortho-positronium into para-positronium [2, 7]. Probabilities of pick-off and ortho–para conversion are dependent on tissue structure and metabolism, respectively, and could provide information about the disease progression, as described in more detail in [5, 7]. Feasibility of employing these phenomena to determine positronium images was evaluated in [3, 4]. Later, the first *ex vivo* study was conducted using a phantom with cardiac myxoma and healthy adipose tissues [2]. Results have shown differences in mean ortho-positronium lifetimes between healthy and cancerous tissues [2, 5, 15]. This observation indicates that positronium imaging may increase specificity of medical imaging [2, 5–7, 16]. Recently, statistical methods for positronium imaging were proposed [17, 18] and it was argued that the total body PET systems (both based on crystals [19–22] and plastics [8]) may be used for effective positronium imaging in clinics [6, 23].

In order to apply positronium imaging in medical practice, it is crucial to elaborate a method for assessment of the precision of the multi-photon PET systems for the positronium lifetime determination.

$\beta+$ emitters, such as ^{18}F, are the most commonly used isotopes in preparation of phantoms for the current PET systems adjusted for registration of double annihilation photons coincidences. However, for the purpose of positronium imaging, it is important to use a $\beta+$ emitter that is capable of sending additional prompt gamma quanta. For the positronium imaging in clinics, ^{44}Sc, ^{68}Ga, or ^{82}Rb are considered [23–25].

Recently, certified materials were suggested for verifying the accuracy of positronium imaging [26]. Here, we propose a phantom for positronium imaging that will contain volumes with different set mean lifetimes of ortho-positronium. It will allow for simultaneous determination of annihilation density distribution and mean positronium lifetimes for specific voxels of activity. The proposition of such a phantom is presented along with prelim-

inary results of a mean ortho-positronium lifetime in the XAD4 [27] water mixtures, that will be used to fill the high-activity volumes in the NEMA IEC phantom [28]. It is also worth considering if such a new phantom would provide some new insight into the currently developed positronium image reconstruction and analysis algorithms [2, 9, 17, 18, 29–31].

2. Positronium imaging phantom concept

The proposed phantom will consist of six volumes of high-activity accumulation immersed in the lower-activity background. Each of the six volumes will exhibit the same activity accumulation and a different mean lifetime of ortho-positronium as presented in figure 1. This will be accomplished by controlling the ortho-positronium lifetime by creating mixtures of the XAD4 polymer and aqueous isotope solution in different proportions. The expected mean lifetime of ortho-positronium in studied mixtures will be assessed by the means of the PALS technique. In the final phantom construction, the desired values of the mean ortho-positronium lifetimes will be obtained by choice of the proper concentration of the XAD4 sample in water.

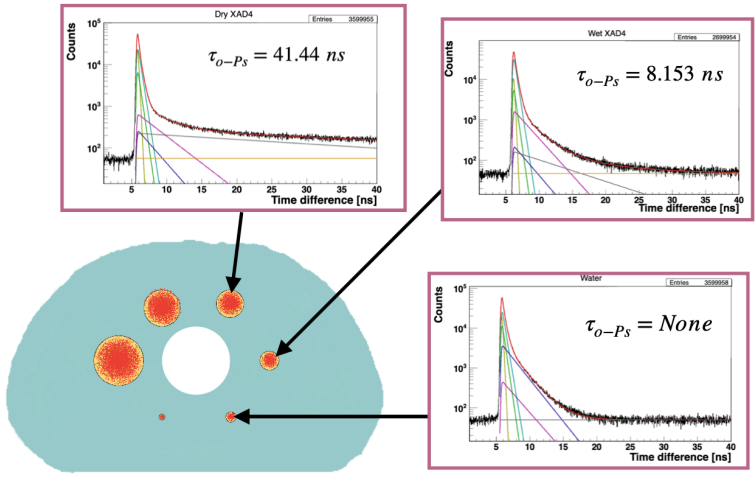

Fig. 1. The proposition of NEMA-like [28] phantom for assessment of the precision of the J-PET positronium imaging method. For each of the volumes, there is the same activity concentration but different mean lifetimes of ortho-positronium (arrows pointing to the different lifetime spectra). The spectra show the results of the measurements described in the text. They were determined for different mass percentages of the XAD4 in water, from the analysis of the respective PAL spectrum. The mass percentage of XAD4 was equal to 100%, 46%, and 0% for upper-left , upper-right, and lower-right spectrum, respectively. $\tau_{\text{o-Ps}}$ indicate mean ortho-positronium lifetimes extracted from the measurement by using the PALS Avalanche program [29]. The fit components are explained in Section 4.

3. Ortho-positronium lifetime

The results of this study were obtained by using the Positronium Annihilation Lifetime Spectroscopy (PALS) method. Measurement of the mean lifetime of positronium is a subject of research of both positronium imaging and the PALS methods. In those methods, it is essential to use $\beta+$ isotopes that after the emission of positron can emit an additional photon, often referred to as a prompt photon, used for setting a reference time for positron lifetime estimation for a single event. In such cases, collected time differences between registration of the annihilation and prompt photons constitute the positron lifetime spectrum. ^{22}Na was used as a $\beta+$ emitter in the conducted research. Its decay scheme, alongside the scheme of the measurement on the time scale, is shown in figure 2 [3–5, 32]. In this study, data for 3.6 million events were collected in each measurement.

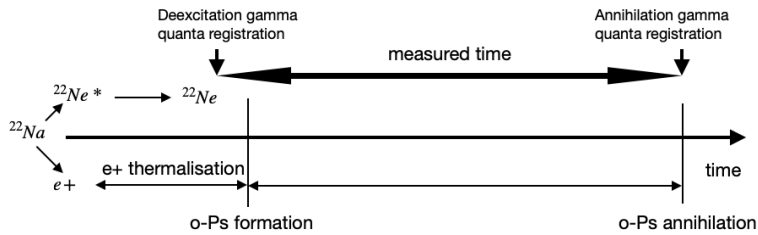

Fig. 2. The order of processes in a single event used in the PALS and positronium imaging.

4. Experimental setup and measurements

The experimental setup, schematically depicted in figure 3, consisted of two detectors, each composed of BaF_2 scintillation crystal and a photomultiplier. A chamber was placed between the detectors, shifted off their axis by a radius of a crystal scintillator to prevent from registering both annihilation gamma quanta. The bottom detector was registering deexcitation gamma quanta (with the energy of 1274 keV) and the upper detector was registering annihilation gamma quanta (with the energy of 511 keV). To obtain the same gains for the detectors, different voltages were applied to the detectors: 2.5 kV and 2.32 kV for the upper and the bottom detector respectively. Signals were delivered to the LeCroy 608C constant fraction discriminator (CFD), where different thresholds were applied to both signals. For the bottom detector, signals with amplitudes higher than 70 mV were gathered, for the upper detector, signals with amplitudes higher than 14.5 mV were gathered. The coincidence window was set for 110 ns. Data was acquired using the digitizer DRS4. The source, ^{22}Na isotope, was encapsulated in a Kapton foil and sealed additionally with parafilm to prevent the water from the sample from damaging the source.

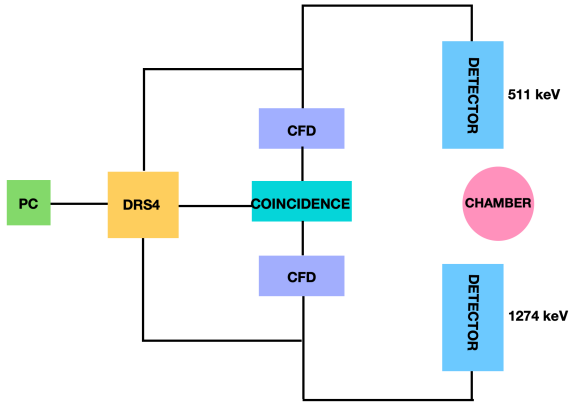

Fig. 3. Scheme of the measurement setup.

In the course of this study, six measurements were done. One measurement of distilled water, one measurement of the dried XAD4, and four measurements of different concentrations of the XAD4 and water. Prepared samples were placed inside aluminium or polytetrafluoroethylene (PTFE) measurement chambers. The obtained data were analysed using the PALS Avalanche program that fits the spectra by a model consisting of a sum of exponential functions used to model a single positron–electron annihilation component convoluted with the Gaussian function reflecting the time resolution [29].

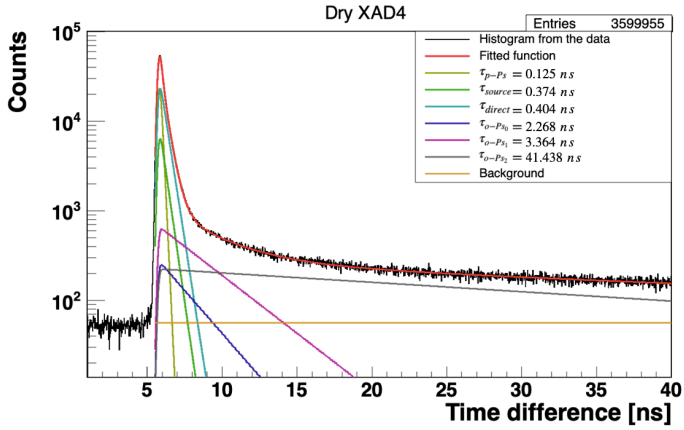

Fig. 4. An exemplary lifetime spectrum determined for the dry XAD4 material. The black histogram shows the experimental data. Superimposed curves indicate the result of the fit. The meaning of the curves is described in the text. The fit was performed from 0 to 110 ns, but for the increased readability of the graph, it is presented in a range from 0 to 40 ns. The background is estimated as a mean of the first 50 values from the left.

In figure 4 exemplary spectrum is presented. Components of the function fitted to this spectrum were as follows: $\tau_{\text{p-Ps}}$ — para-positronium annihilation (lifetime fixed), τ_{source} — positron annihilation in the source (lifetime and intensity fixed), τ_{direct} — positron annihilation in the sample (value of its intensity can change freely and its initial lifetime value can change in the appointed range from 0.32 ns to 0.48 ns), $\tau_{\text{o-Ps0}}$ — ortho-positonium annihilation in parafilm (lifetime and intensity fixed). The values of parameters τ_{source} and $\tau_{\text{o-Ps0}}$ was ascertained in the previous measurements.

Two fully free components were corresponding to ortho-positronium lifetime in XAD4 pores: $\tau_{\text{o-Ps1}}$ and $\tau_{\text{o-Ps2}}$. The values of those two components were hypothesized to change in between the measurements according to the amount of water added to XAD4.

5. Results

In figure 5, the dependencies of the ortho-positronium component with a longer mean lifetime and its respective intensity on a mass percentage of the XAD4 in the mixture are presented. The mean ortho-positronium component with a longer mean lifetime and its intensity are increasing with the XAD4 fraction in the mixture. The red lines in figure 5 are corresponding to the arbitrary models used to fit the experimental results. The measured values of component with longer mean ortho-positronium lifetimes and their respective intensities are presented in Table 1.

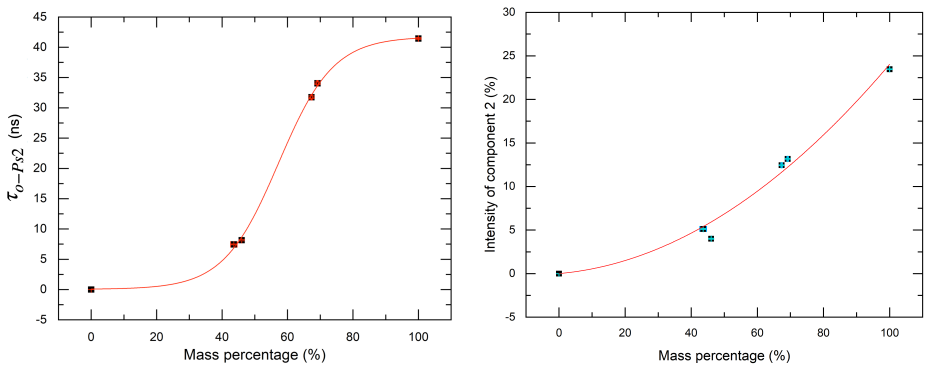

Fig. 5. Left: Dependency of the lifetime of ortho-positronium for the XAD4 second component on the mass percentage of the XAD4 in water. Squares indicate the result of the measurements. The red line is drawn to guide the eye. It corresponds to the function: $y = 20.9 + 20.9 \times \tanh(0.06 \times (x - 57.27))$. Right: Dependency of the intensity of the second component on the mass percentage of the XAD4 in water. Squares indicate the result of the measurements. The red line is drawn to guide the eye. It corresponds to the function: $y = -0.0337 \times x + 0.00207 \times x^2$. The error bars of the values of fitted components are smaller than the point size. Other types of uncertainties were not accounted for in this study.

Table 1. Results of the PALS measurements of lifetime and intensity of the ortho-positronium second component for the XAD4. C_{p} denotes mass percentage of the XAD4 in water and is described by $= m_x/(m_x + m_s) \times 100\%$, where m_x is the XAD4 mass and m_{s} is the solvent mass. χ^2_ν is the goodness of the fit defined as χ^2 per degrees of freedom. Mass percentages of 46% and 43.6% (indicated by *) were estimated based on the initial wetness of the shipped product. The concentration of the rest was based on assumption that the dried XAD4 had a mass percentage of 100%. For the pure water spectrum, there was no second component present in the fit.

C_p [%]	Lifetime [ns]	Intensity [%]	χ^2_ν
0	none	none	1.44
43.6(1.0)*	7.453(75)	5.123(50)	1.24
46*	8.153(99)	4.002(45)	1.26
67.33(23)	31.76(22)	12.447(39)	1.38
69.16(23)	34.06(22)	13.170(38)	1.34
100	41.44(17)	23.467(40)	1.34

6. Conclusions

The obtained results indicate that there is a correlation between mean lifetime of ortho-positronium in pores of the XAD4 and the mass percentage of the XAD4 in water. Additionally, the correlation between the intensity of the longer second component and mass percentage of XAD-4 in water was also established.

Those results can be used to prepare a NEMA-like phantom for measurements of the ortho-positronium lifetime alongside the activity concentration that may serve for the assessment of PET systems for positronium imaging.

Authors acknowledge the support of the Foundation for Polish Science through the programme TEAM POIR.04.04.00-00-4204/17; the National Science Centre, Poland (NCN) through grants Nos. 2021/42/A/ST2/00423 and 2021/43/B/ST2/02150; the Ministry of Education and Science under grant No. SPUB/SP/530054/2022; E.U. Horizon 2020 research and innovation programme, STRONG-2020 project, under grant agreement No. 824093; the Jagiellonian University via the project CRP/0641.221.2020, and via SciMat and qLife Priority Research Areas under the Strategic Programme Excellence Initiative at the Jagiellonian University.

REFERENCES

[1] P. Moskal, *IEEE Nucl. Sci. Symp. Med. Imaging Conf. (NSS/MIC)* **2019**, 1 (2019).

[2] P. Moskal *et al.*, *Sci. Adv.* **7**, eabh4394 (2021).

[3] P. Moskal *et al.*, *EJNMMI Phys.* **7**, 44 (2020).

[4] P. Moskal *et al.*, *Phys. Med. Biol.* **64**, 055017 (2019).

[5] P. Moskal *et al.*, bioRxiv the preprint Server for Biology, 2021, DOI: 10.1101/2021.08.05.455285.

[6] P. Moskal, E. Stępień, *Front. Phys.* **10**, 891 (2022).

[7] P. Moskal *et al.*, *Nat. Rev. Phys.* **1**, 527 (2019).

[8] S. Niedźwiecki *et al.*, *Acta Phys. Pol. B* **48**, 1567 (2017).

[9] P. Moskal *et al.*, *Nat. Commun.* **12**, 1 (2021).

[10] M.D. Harpen, *Med. Phys.* **31**, 57 (2003).

[11] R. Garwin, *Phys. Rev.* **91**, 1571 (1953).

[12] P. Stepanov *et al.*, *Phys. Chem. Chem. Phys.* **22**, 5123 (2020).

[13] K. Shibuya *et al.*, *Commun. Phys.* **3**, 173 (2020).

[14] M. Zare *et al.*, *Radiat. Phys. Eng.* **3**, 1 (2022).

[15] B. Jasińska *et al.*, *Acta Phys. Pol. B* **48**, 1737 (2017).

[16] P. Moskal, E. Stępień, *Bio-Alg. Med-Sys.* **17**, 311 (2021).

[17] J. Qi, B. Huang, *IEEE Trans. Med. Imaging* **41**, 2848 (2022).

[18] Z. Zhu, C.-M. Kao, H.-H. Huang, arXiv:2206.06463 [physics.med-ph].

[19] B.A. Spencer *et al.*, *J. Nucl. Med.* **62**, 861 (2021).

[20] J.S. Karp *et al.*, *J. Nucl. Med.* **61**, 136 (2020).

[21] I. Alberts *et al.*, *Eur. J. Nucl. Med. Mol. Imaging* **48**, 2395 (2021).

[22] G.A. Prenosil *et al.*, *J. Nucl. Med.* **63**, 476 (2022).

[23] P. Moskal, E. Stępień, *PET Clinics* **15**, 439 (2020).

[24] T. Matulewicz, *Bio-Alg. Med-Sys.* **17**, 235 (2021).

[25] J. Choiński, M. Łyczko, *Bio-Alg. Med-Sys.* **17**, 241 (2021).

[26] S. Takyu *et al.*, *Appl. Phys. Express* **15**, 106001 (2022).

[27] https://www.sigmaaldrich.com/specification-sheets/304/271/XAD4-BULK_____SIGMA____.pdf

[28] https://capintec.com/product/nema-iec-pet-body-phantom-set/

[29] K. Dulski, *Acta Phys. Pol. A* **137**, 167 (2020).

[30] R. Shopa *et al.*, submitted to *Bio-Alg. Med-Sys.*

[31] K. Shibuya *et al.*, *Phys. Med. Biol.* **67**, 025009 (2022).

[32] D. Kamińska *et al.*, *Eur. Phys. J. C* **76**, 1 (2016).